Energy 158 (2018) 986–1000

Contents lists available at ScienceDirect

Energy

journal homepage: www.elsevier.com/locate/energy

Energy and exergy analysis of reciprocating natural gas expansion engine based on valve configurations

Mohsen Jannatabadi [a, *], Mahmood Farzaneh-Gord [b], Hamid Reza Rahbari [c], Abolfazl Nersi [d]

[a] Minoodasht Branch, Islamic Azad University, Minoodasht, Iran
[b] Faculty of Engineering, Mechanical Engineering Department, Ferdowsi University of Mashhad, Mashhad, Iran
[c] The Faculty of Mechanical Engineering, Shahrood University of Technology, Shahrood, Iran
[d] Technical Inspection Supervisor, Golestan Gas, NIGC, Iran

ARTICLE INFO

Article history:
Received 23 October 2017
Received in revised form
21 May 2018
Accepted 16 June 2018
Available online 18 June 2018

Keywords:
Natural gas pressure reduction
Genetic algorithm
Expansion engine
Power generation
Exergy efficiency

ABSTRACT

Natural gas pressure should be reduced in city gate stations before consuming. Part of the physical exergy of this high pressure gas is wasted if throttling valves are employed for pressure reduction. Reciprocating natural gas expansion engine (RNGEE) could be utilized to recover most of the physical exergy. In this study, a single acting RNGEE is investigated thermodynamically in order to optimize the ports opening/closing times. For this purpose, cylinder and slide valves and two types of piston valves have been modeled and compared. Based on an exergy analysis, a genetic algorithm has been developed to optimize the valves timing. Moreover, effects of the pressure ratio on the exergetic efficiency and power generation of the RNGEE have been studied numerically. Methane was modeled as a real gas by employing AGA8 equation of state. Results showed that beside importance of exergy efficiency optimization, inlet process period has also critical impacts on engine performance. Moreover, power generation is almost the same while using cylinder or flange valves (~1986 kW/kg) with exergy efficiencies of 83.6% and 82.7% respectively. In contrast, slide and piston valves are found to have lower power generation (1746 kW/kg and 1753 kW/kg respectively) with the exergy efficiency of ~72%.

© 2018 Elsevier Ltd. All rights reserved.

1. Introduction

Natural gas (NG) extracted from refinery has a high pressure of about 70 bars. In order to transport this high pressure gas to a distribution system where it is being consumed, its pressure should be reduced to a safe and usable level. This is usually done in natural gas pressure reduction stations which sometimes called city gate stations (CGSs). Nowadays In most of countries, throttling valves are used to reduce the gas pressure [1] where the physical exergy of high pressure gas is wasted.

To reduce the amount of exergy destruction, a few configuration has been proposed to be employed in CGSs. A Combined Heat and Power (CHP) system could be employed in CGS for necessary pre-heating as well as generation the power. A CHP system has been optimized with genetic algorithm (GA) by Sanaye [2]. It was found that the payback period of the investment is 1.23 years. Some CHP technologies such as turbines, rotary and screw expanders have been studied with Badr et al. [3] they have analyzed parameters such as power output, rotational speed. Objective function of actual annual benefit in terms of dollar in natural gas pressure reduction stations has been maximized by Sanaye and Nasab [4] with GA. Results showed that ambient conditions and pressure & mass flow rate of the inlet natural gas has a significant role in selecting the appropriate method for pressure reduction systems. Farzaneh-Gord et al. [5] have analyzed solar heater installation in CGSs through energy and exergy point of view.

There are number of studies on recovering physical exergy of high pressure natural gas during pressure reduction mostly focusing on the pressure exergy recovering devices. The turbo expander and RNGEE are two candidate devices. Bisio has proposed using the mechanical systems to convert pressure exergy of NG into compressed air [6]. Neseli carried out a study focusing on installing turbo expander instead of throttling valve in Izmir [7]. It was shown by Kostowski and Usón [8] that expansion systems such as turbo expander could provide mechanical energy to drive electric

* Corresponding author.
E-mail addresses: m.jannatabadi@minoodashtau.ac.ir (M. Jannatabadi), mahmood.farzaneh@yahoo.co.uk (M. Farzaneh-Gord), rahbarihamidreza@yahoo.com (H.R. Rahbari), abolfazl.nersi@gmail.com (A. Nersi).

https://doi.org/10.1016/j.energy.2018.06.103
0360-5442/© 2018 Elsevier Ltd. All rights reserved.

generators. Pressurized gas contains physical exergy could be converted to electricity or may even be utilized directly in particular industrial applications. Kolasinski et al. [9] presented an analytical modeling of rolling piston expander in natural gas expansion due to pressure reduction of NG. They have stated advantages of these expanders against to turbines which are more complicated and expensive. Their results showed the effect of varied sizes of the expander components and natural gas thermal properties at the inlet and outlet of the expander and the expander output power.

In addition of turbo expander, RNGEE could be employed to recover this wasted energy. Fig. 1 shows that RNGEE could be installed in parallel with expansion valve. It can be said using of RNGEE is one of the newest method to recovering and producing energy without any fuel consumption.

Although, there could be a lot of use for NG expansion, to the best of our knowledge, there are not enough academic studies, especially in area of RNGEE. In a report by Dehli [10], using of RNGEE for power generation from natural gas pressure reduction has been introduced. He has shown that, the amount of electrical power generation is depended on the level of inlet temperature, the mass flow rate and the pressure ratio. Effects of geometrical parameters on the rates of power generation and RNGEE performance have been studied by Farzaneh-Gord and Jannatabadi [11]. In another study, Farzaneh-Gord and Jannatabadi [12] studied timing optimization of RNGEE treating methane as an ideal gas. They have studied cylinder valve and shown that exergy destruction due to mixing and heat transfer could be neglected. Moreover, they have shown that pressure ratio has a strong effect on timing optimization too. Farzaneh-gord et al. [13] have studied also the expander installation in town border stations. It was found that the initial investment will be returned after 1.5 years.

Exergy analysis could be used to calculate the amount of RNGEE power generation or amount of work lost [14]. An expansion engine is very similar to a reciprocating compressor, however the work cycle is reverse, consequently studies on reciprocating compressor could be used to model RNGEE [12]. Several sources of exergy destruction have been modeled by different researchers. McGovern and Harte [15] and [16] have identified the exergy destruction sources of compressor and have showed that exergy destruction due to heat transfer and mixing could be neglected in reciprocating compressor.

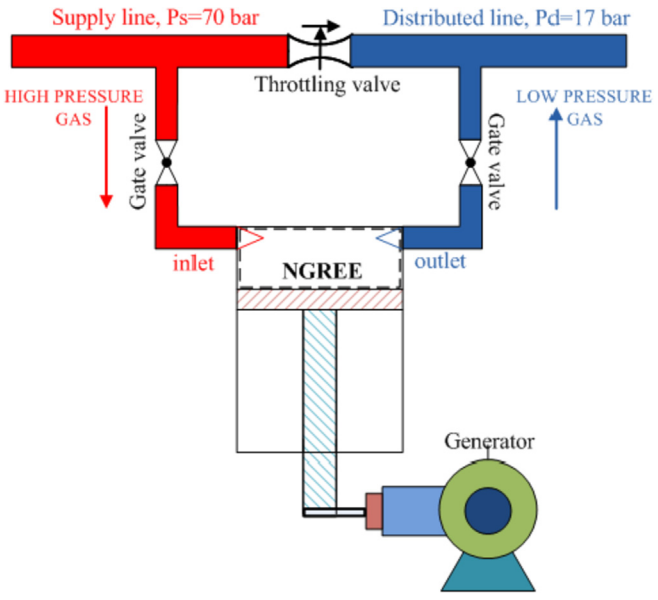

Fig. 1. Installing RNGEE in CGS.

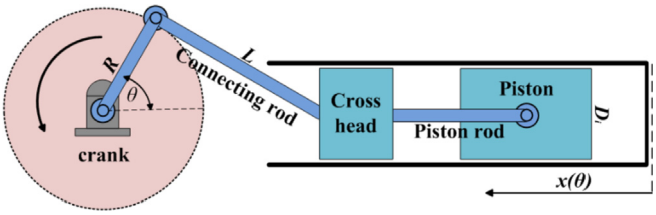

Fig. 2. Slider crank mechanism.

Although, there have been a lot of exergy lost in CGSs but so far a few studies have been carried out to design and optimize RNGEE. In last studies [11] and [12], a single acting expansion engine with just a cylinder valve has been introduced. The effect of geometrical parameters of engine for a sample timing has been simulated in Ref. [11] and in Ref. [12] the effect of these parameters on timing optimization of ports has been shown. In both of these studies the methane has been modeled as an ideal gas. But in this study, the thermodynamic analysis including continuity equation, energy balance and exergy analysis have been used to study a single acting RNGEE and methane is modeled as a real gas. For small scale power generation, turbine should not be used due to complexity and cost [17], but RNGEE could be used for any scale of power reduction. Then for first time, the RNGEE with four different valve configurations in natural gas pressure reduction stations has been studied aiming to recover physical exergy of high pressure natural gas. These four valves are categorized in cylinder, slide, piston and flange types. In this analysis, two valves are moved over two inlet/outlet ports in the cylinder valve, but in other types, a single valve is moved over a port. To calculate exergy flows and exergy lost resources, exergy analysis was used and to obtain optimum timing of ports opening/closing times, exergy efficiency is selected as a fitness function which is maximized using a modified elite genetic algorithm. Also the effect of inlet pressure variation on engine performance has been stated for the first time in this paper.

2. Methodology

RNGEE in-cylinder gas is assumed as control volume for thermodynamic modeling. The model could measure and predict all thermodynamic properties in the expansion chamber as a function of crank angle. The advance numerical simulation model is based on transient governing equations of the continuity and energy (Fig. 2).

2.1. Piston displacement

To convert straight-line motion of mechanical parts to rotary motion, as in a RNGEE, slider crank mechanism should be used [12].

In order to convert all differential equation respect to time to the form of crank angle below equation is used [18]:

$$\frac{d}{dt} = \frac{d}{d\theta}\frac{d\theta}{dt} = \omega\frac{d}{d\theta} \tag{1}$$

Instantaneous piston displacement according to top dead center (TDC) and gas volume can be measured as follows [11]:

$$x(\theta) = x_{cl} + R(1-\cos\theta) + L\left\{1 - \sqrt{1 - \left(\frac{R}{L}\right)^2 \sin^2\theta}\right\} \tag{2}$$

$$V_{cv}(\theta) = x(\theta)\pi\frac{D_i}{4} \tag{3}$$

2.2. First law of thermodynamics

To develop a numerical method, conservation of mass and first law of thermodynamic have been applied on gas inside the cylinder. With neglecting kinetic and potential energies terms in the inlet and outlet enthalpy fluxes and assuming that energy is just a function of internal energy, first law of thermodynamic in a rate format could be presented as follows [12]:

$$\frac{d(mu)_{cv}}{d\theta} = \frac{dQ_{cv}}{d\theta} - \frac{dW_{cv}}{d\theta} + \frac{dm_s}{d\theta}h_s - \frac{dm_d}{d\theta}h \tag{4}$$

Where the work term could be computed according to the following equation [12]:

$$\frac{dW_{cv}}{d\theta} = P_{cv}\frac{dV_{cv}}{d\theta} \tag{5}$$

2.3. Continuity equation

Continuity equation could be presented as below [12]:

$$\frac{dm_{cv}}{d\theta} = \frac{dm_s}{d\theta} - \frac{dm_d}{d\theta} \tag{6}$$

Where the mass flow rate through inlet and outlet ports are simulated as orifices and for real gas could be calculated from following equations [19]:

$$\frac{dm}{d\theta} = \begin{cases} \frac{1}{\omega}A(\theta)P_{us}C_d\sqrt{\frac{2\gamma}{(\gamma-1)R_gT_{us}}}\sqrt{\left(\frac{P_{ds}}{P_{us}}\right)^{\frac{2}{\gamma}} - \left(\frac{P_{ds}}{P_{us}}\right)^{\frac{\gamma+1}{\gamma}}} & if\ \frac{P_{ds}}{P_{us}} > \left(\frac{2}{\gamma+1}\right)^{\frac{\gamma}{\gamma-1}} \\ \frac{1}{\omega}A(\theta)P_{us}C_d\sqrt{\frac{\gamma}{R_gT_{us}}\left(\frac{2}{\gamma+1}\right)^{\frac{\gamma+1}{\gamma-1}}} & if\ \frac{P_{ds}}{P_{us}} \le \left(\frac{2}{\gamma+1}\right)^{\frac{\gamma}{\gamma-1}} \end{cases} \tag{7}$$

The second equation in each formula is related to chocking effect when gas through ports reaches the speed of sound. In these equations, C_d is the discharge coefficient. C_d could be treated as a coefficient which stand for non-ideality of the gas flow through the orifice. For simple pressure loss or flow rate calculations where high accuracy is not critical, typical values of discharge coefficient may be used. These typical values are in the range between 0.61 and 0.984, which depends on the geometry of the Orifice and the type of equipment used [20]. It should be noted that the amount of A is depended on configuration of valve, which will be explained in next section. Subtitle of us is defined up stream and ds is defined down stream of gas flow.

2.4. Instantaneous port area equations and valve configurations

Valve timing is a system applied to compute instantaneous valve operation according to crankshaft position in degrees. As mentioned before, four valves types as; cylinder, slide and two types of piston valves are modeled theoretically. At first, it is necessary to mention that in all valve types, an intake port opening time (IPOT) is set at the beginning of a cycle (here zero degrees of crank revolution or TDC). Also it was assumed there are several rectangular slots on the cylinder wall of each valve chest which these slots are separated with bridges. All slots and bridges are assumed as a port.

2.4.1. Cylinder valve configuration (CVC)

As shown in Fig. 3, two valve chests and therefore, two ports are considered for CVC, one for inlet and other for outlet. In all valve types the port length could be obtained as follows:

$$L_p = \pi D_v - n_b w_b \tag{8}$$

Where D_v is valve chest diameter, n_b is the number of bridges, and w_b is bridge width. Then the port area would be calculated as an area of rectangular:

$$A_{CVC} = L_p W_p \tag{9}$$

Which W_p is port width. By consideration equation (7), following sine functions are used to control instantaneous cross section area of mass flow in CVC:

$$\text{For inlet: } A_s(\theta) = A_{CVC}\sin\left(\frac{\theta}{\theta_0}\pi\right)\ if\ 0 \le \theta \le \theta_0 \tag{10}$$

$$\text{For outlet: } A_d(\theta) = A_{CVC}\sin\left(\frac{\theta-\theta_i}{\theta_e-\theta_i}\pi\right)\ if\ \theta_i \le \theta \le \theta_e \tag{11}$$

As it can be seen from above relations, both inlet and outlet ports will be begun to close immediately after they are opened fully. In this model both ports will be fully opened. This style of valve can be controlled electronically, so opening/closing timing of ports could be changed according to inlet conditions.

2.4.2. Flange valve configuration (FVC)

In first type of piston valve (here called flange valve), Fig. 4, the instantaneous inlet port area is same as CVC, Eq. (10), but for outlet port, following equation is used:

$$\text{For outlet: } C_d = \begin{cases} \sin\left(\frac{\theta-\theta_i}{\theta_1-\theta_i}\frac{\pi}{2}\right) & if\ \theta_i \le \theta < \theta_1 \\ 1 & if\ \theta_1 \le \theta < \theta_2 \\ \sin\left(\frac{\theta-\theta_2}{\theta_e-\theta_2}\frac{\pi}{2}\right) & if\ \theta_2 \le \theta \le \theta_e \end{cases} \tag{12}$$

In this case, one port is used for both gas inlet and outlet. In equations (10) to (12), θ_0 stands for an intake port closure time (IPCT), θ_i is an exhaust port opening time (EPOT), θ_1 is the time of exhaust port, which is fully opened (EPFO), θ_2 is the time which exhaust port begins to close (EPBC). This means that the port will be

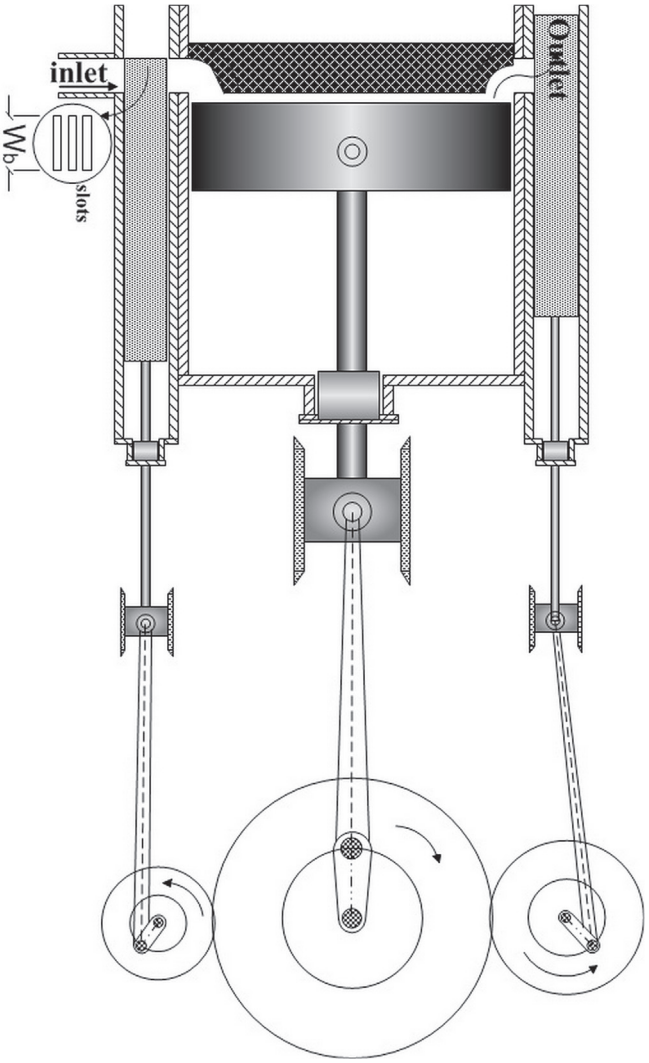

Fig. 3. A schematic of cylinder valve configuration.

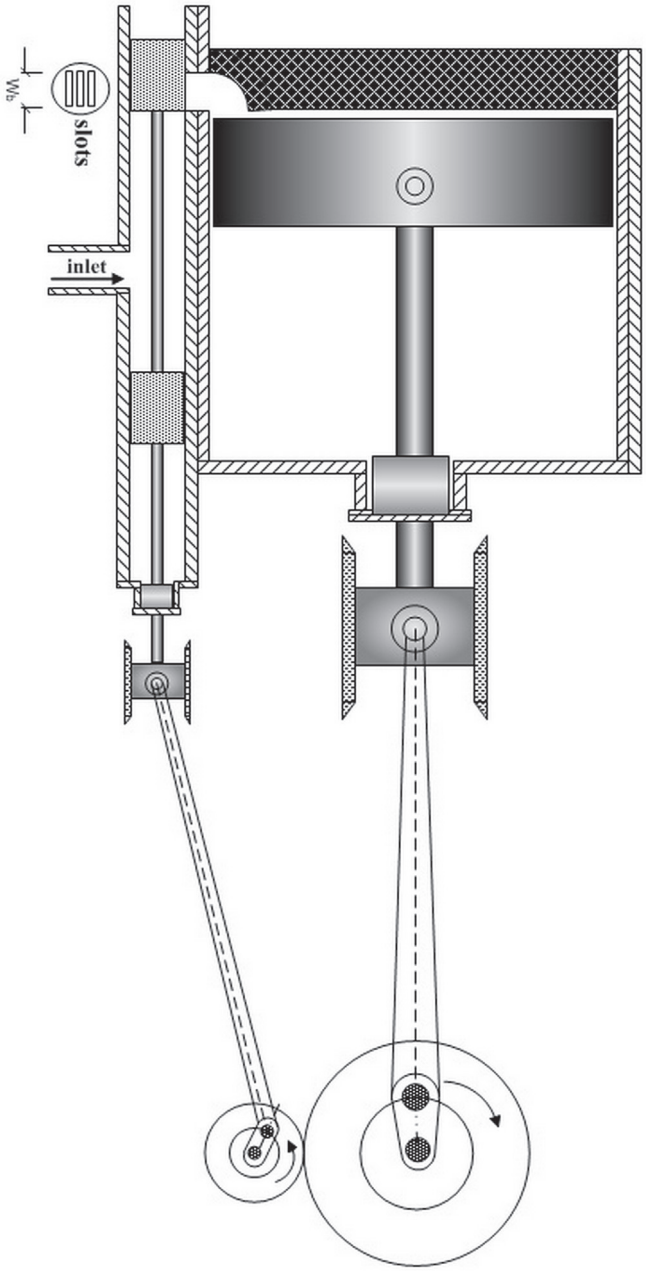

Fig. 4. A schematic of flange valve configuration.

remained open from θ_1 to θ_2. Finally, θ_e is the exhaust port closure time (EPCT).

2.4.3. Slide valve configuration (SVC)

SVC has a flat sliding face and is called "outside admission" too, means that pressurized inlet gas enters from around the outside of the valve and exhausts through the middle of the valve, Fig. 5. A rectangular port with a length equals to the piston diameter is selected. An eccentric is used to drives the valve back and forth. The point, at which the inlet port is closed, is called "cut-off." The position of the valve "events" and the duration that the ports are opened and closed depends on the cut-off setting of the valve gear.

In SVC, Lead is the length of port that the valve opens before the piston reaches a dead center. When the valve is in its mid-stroke, inlet/exhaust lap is the distance that the valve head overlaps the inlet/outlet side of the port, respectively. The valve displacement from its mid position is given as [21]:

$$z = r_{eq} \sin(\theta + \psi) \tag{13}$$

In this equation, r_{eq} is eccentric crank radius (constant), it is evident that valve stroke is twice of r_{eq}, θ is crank angle and ψ is the eccentric angle of advance (constant). At TDC ($\theta = 0$), at the beginning of inlet stroke, the port is opened by an amount of lead (L_e), so that [21]:

$$S_l + L_e = r_{eq} \sin(\psi) \tag{14}$$

Where S_l is inlet lap. According to crank angle of cut-off, θ_c, the displacement of the valve from its mid-point is equal to inlet lap, so it can be achieved that:

$$S_l = r_{eq} \sin(\theta_c + \psi) \tag{15}$$

From these relations, it follows:

$$\psi = \tan^{-1}\left[\sin\theta_c \Big/ \left(\frac{S_l}{S_l + L_e} - \cos\theta_c\right)\right] \tag{16}$$

According to these definitions, the instantaneous port openings can be expressed as:

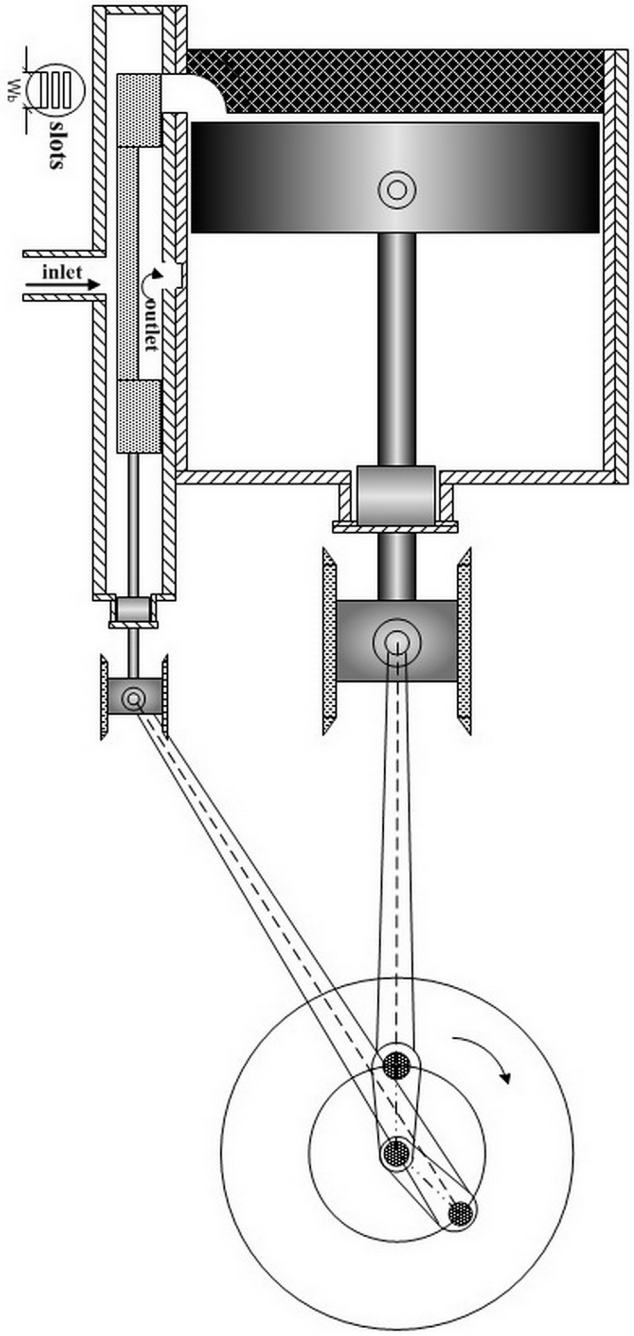

Fig. 5. A schematic of slide valve configuration.

$$y_i = r_{eq}\sin(\theta+\psi) - S_l \tag{17}$$

$$y_o = -r_{eq}\sin(\theta+\psi) - E_l \tag{18}$$

2.4.4. Piston valve configuration (PVC)

A piston valve has two piston-shaped heads as shown in Fig. 6. It should be noted, unlike SVC, for a piston valve, high pressure gas enters through the inside of the valve and exhausts through the outside. Below equations are used for PVC:

$$z = r_{eq}\sin(\theta-\psi) \tag{19}$$

$$S_l + L_e = r_{eq}\cos(-\psi) \tag{20}$$

$$S_l = r_{eq}\sin(\theta_c-\psi) \tag{21}$$

$$\psi = \tan^{-1}\left[\left(\frac{S_l}{S_l+L_e} - \cos\theta_c\right)\Big/\sin\theta_c\right] \tag{22}$$

$$y_i = r_{eq}\cos(\theta-\psi) - S_l \tag{23}$$

$$y_o = -r_{eq}\cos(\theta-\psi) - E_l \tag{24}$$

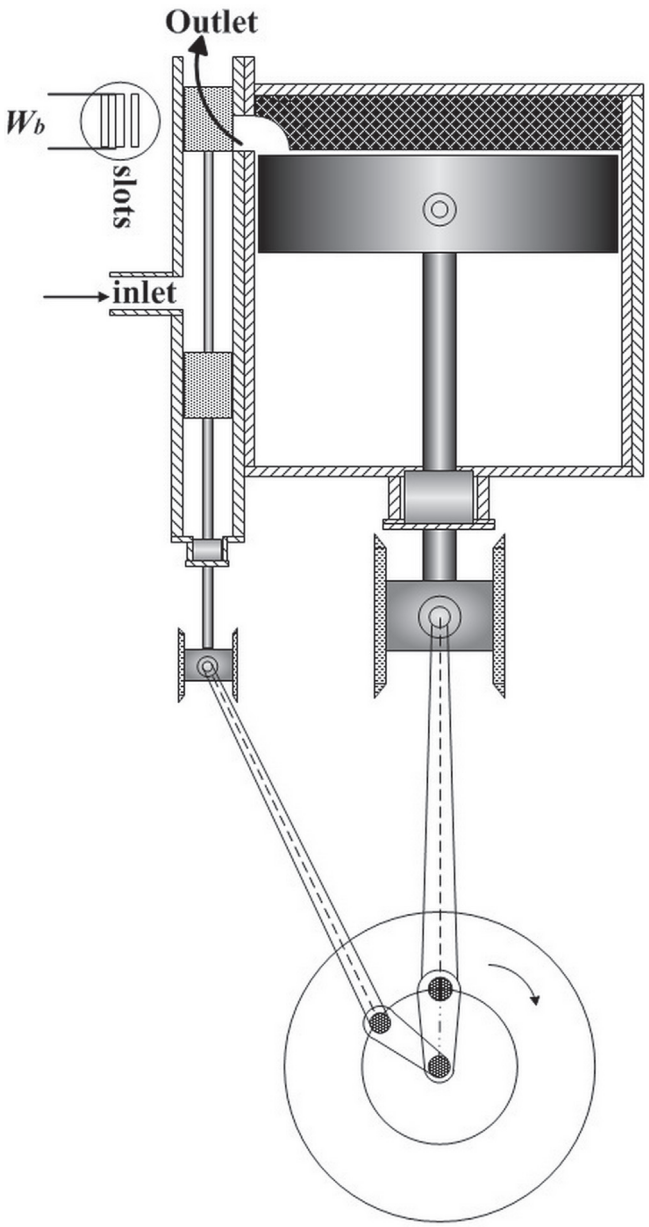

Fig. 6. A schematic of piston valve configuration.

2.5. Heat transfer equations

In RNGEE, heat transfer occurs between gas and cylinder wall which for simplicity, cylinder wall temperature is considered constant and is measured as $(T_s + T_d)/2$ [18]. Due to prolonged outlet process of gas in RNGEE, outlet temperature unlike inlet temperature is not constant and calculated as follows [12]:

$$T_d = \frac{\sum(m_d T_{cv})}{\sum m_d} \tag{25}$$

According to overall heat transfer coefficient, following equation can be used for calculating instantaneous heat transfer between cylinder wall and in-cylinder gas temperature [18]:

$$Q_{cv}(\theta) = U(\theta)A(\theta)(T_{cv}(\theta) - T_w) = \frac{(T_{cv}(\theta) - T_w)}{R_i} \tag{26}$$

$A(\theta)$, total heat transfer area, is surface area in contact with the gas which is related to piston and cylinder head area and instantaneous area of the wall cylinder. The same equation as equation (26) are applied for modeling heat lost in internal combustion engine or reciprocating compressors.

2.6. Works equations

The equation of friction lost is given by Ref. [12]:

$$W_f = 2S\pi f P_{cv}(\theta) L_r D_i \tag{27}$$

where L_r is the ring width, f is the friction coefficient of glass filled PTFE material. The indicated work is obtained with:

$$W_{cv} = \int_{\theta=0}^{\theta=360} P_{cv} dV_{cv} \tag{28}$$

So brake work would be measured as follows:

$$W_b = W_{cv} - W_f \tag{29}$$

3. Exergy analysis

It can be said that exergy analysis is a powerful method in thermodynamic optimization of system processes [22] [23] [24] [25]. Identifying the sources of exergy losses is caused to improve system [26]. RNGEE is an open system, so according to [27] and [28] at the steady state, the rate of exergy transfer to a system is obtained with:

$$\dot{\Xi}_t = \dot{m}(b_s - b_d) = \dot{m}_s(h_s - T_0 s_s) - \dot{m}_d(h_d - T_0 s_d) \tag{30}$$

Where $\dot{\Xi}_t$ represents the rate of exergy transfer, T_0, $\dot{m}$, h and s is the ambient temperature, mass flow rate, enthalpy and entropy respectively. In RNGEE, exergy efficiency can be measured as a ratio of brake power to exergy decrease of the incoming and outgoing flows:

$$\Psi = \frac{\dot{W}_b}{\dot{\Xi}_t} \tag{31}$$

$\dot{W}_b$ is called “desired exergy output” or “product” and $\dot{\Xi}_t$ is called “exergy used” or “fuel” [12], [29] and [30]. Inlet/outlet throttling, friction, mixing of inlet gas with in-cylinder gas and heat transfer between inside gas and environment are exergy loss sources in RNGEE.

3.1. Exergy destruction due to throttling

It occurs an adiabatic throttling through fluid passing to and from the control volume. In the following equations, both inlet and outlet throttling are given respectively [15] and [29].

$$\dot{I}_{th_s} = T_0 \dot{m}_s [s'_s - s_s] \tag{32}$$

$$\dot{I}_{th_d} = T_0 \dot{m}_d [s_d - s_c] \tag{33}$$

In first equation, s'_s is specific entropy after throttling, which is calculated at inlet enthalpy and in-cylinder gas pressure.

3.2. Exergy destruction due to heat transfer

The irreversibility rate due to heat transfer from bulk temperature of T_{cv} to the wall cylinder with temperature of T_w is given by Refs. [12] and [31]:

$$\dot{I}_{Q_{cv}} = T_0 \dot{Q}_{cv} \left(\frac{1}{T_{cv}(\theta)} - \frac{1}{T_w} \right) \tag{34}$$

3.3. Exergy destruction due to mixing

There is the other cause of exergy lost due to mixing of throttled fluid with temperature of T'_i with in-cylinder gas temperature [15]. An exergy destruction rate will be occurred due to the exergy transfer rate from the inlet gas and exergy transfer rate to the control volume as [15]:

$$\dot{I}_{mix} = \int_{T'_s}^{T_{cv}} \delta \dot{I} = \dot{m}_s T_0 \left((s_{cv}(\theta) - s'_s) - \frac{h_{cv}(\theta) - h_s}{T_{cv}(\theta)} \right) \tag{35}$$

Then it can be said that total exergy destruction of flowing gas through RNGEE is calculated as follow:

$$\dot{I}_{total} = \dot{I}_{th_s} + \dot{I}_{th_d} + \dot{I}_{Q_{cv}} + \dot{I}_{mix} + \dot{I}_{fr} \tag{36}$$

Total exergy destruction can be obtained through the second law of thermodynamic too [14].

$$\dot{I}_{total} = T_0 \dot{S}_{gen} \tag{37}$$

Total entropy generation rate, $\dot{S}_{gen}$, is achieved with integration of below equation:

$$\dot{S}^{j+1}_{gen} \Delta\theta = m^j_c \left(s^{j+1}_c - s^j_c \right) + s^j_c \left(\dot{m}^{j+1}_s - \dot{m}^{j+1}_d \right) + \dot{m}^j_d s_d \Delta\theta - \dot{m}^j_s s_s \Delta\theta - \frac{\left(T_w - T^j_c \right)}{R^j_i T^j_c} \Delta\theta \tag{38}$$

4. Thermodynamic properties of methane as natural gas

Knowing thermodynamic properties of natural gas is vital for analyzing RNGEE. The current study has employed a numerical procedure for computing all needed thermodynamic properties of

NG based on AGA8 standard, which has been presented by American gas association, specifically for computing compressibility factor and density of natural gas.

In this study, NG is considered as real gas of methane. Obviously due to measuring all control volume thermodynamic properties, two independent properties are needed. These two properties are internal energy, which is obtained from first law of thermodynamic and density, which can be computed from conservation of mass. For more information refer to [32].

4.1. AGA8 equation of state

The basic form of AGA8 equation of state is given by Ref. [33]:

$$P_{cv} = Z\rho_m RT_{cv} \tag{39}$$

ρ_m is molar density and Z is the compressible factor which can be related through the following equation:

$$Z = 1 + B\rho_m - \rho_r \sum_{n=13}^{18} C_n^* + \sum_{n=13}^{58} C_n^* D_n^* \tag{40}$$

$\rho_r = K^3\rho_m$ is reduced density. More information about computing constants and other parameters are given in Refs. [32] and [33]. With having gas pressure and temperature and replacing equation (40) into (39), it can be seen that just molar density is unknown parameter, which is calculated by an iterative method of Newton-Raphson [32]. In the following relations enthalpy, internal energy and entropy will be given as a function of temperature and molar density [34].

4.2. Enthalpy computation

The residual enthalpy equation is written as [34]:

$$h_m = h_{m,I} - RT_{cv}\int_0^{\rho_m}\left(\frac{\partial Z}{\partial T}\right)_{\rho_m}\frac{d\rho_m}{\rho_m} + RT_{cv}\int_0^1 dZ \tag{41}$$

In above equation, h_m is a molar enthalpy for real gas and $h_{m,I}$ is a molar enthalpy for ideal gas, which will be introduced as follows [32]:

$$h_{m,I} = h_{m,i0} + a^*T_{cv} + b^*c^*\coth\left(\frac{c}{T_{cv}}\right) - d^*e^*\tanh\left(\frac{e}{T_{cv}}\right) \tag{42}$$

The term of $h_{m,i0}$ is an enthalpy for methane as an ideal gas in the reference state of $25^\circ C$ and 101.325 kPa which the method of its calculation and other constant parameters for methane is given in Ref. [35].

4.3. Internal energy computation

A function of internal energy residual is given by the relation [34]:

$$u_m = u_{m,I} - RT^2\int_0^{\rho_m}\left(\frac{\partial Z}{\partial T}\right)_{\rho_m}\frac{d\rho_m}{\rho_m} \tag{43}$$

Where u_m indicates the molar internal energy for real gas and $u_{m,I}$ represents the molar internal energy for ideal gas, which is calculated as [32]:

$$u_{m,I} = h_{m,I} - P_{cv}v_m = h_{m,I} - RT_{cv} \tag{44}$$

4.4. Entropy computation

Molar entropy residual function is [34]:

$$s_m = s_{m,I} - R\int_0^{\rho_m}\left[Z + T_{cv}\left(\frac{\partial Z}{\partial T}\right)_{\rho_m}\right]\frac{d\rho_m}{\rho_m} \tag{45}$$

In this equation, $s_{m,I}$ shows the molar entropy for ideal gas and could be obtained as:

$$s_{m,I} = s_{m,i0} + s_{m,I}(T_{cv}) - RLn(P_{cv}) \tag{46}$$

The parameter of $s_{m,i0}$ is the entropy of methane as ideal gas at reference conditions and $s_{m,I}(T_{cv})$ is molar entropy as a function of temperature, which could be calculated as follows [32]:

$$s_{m,I}(T_{cv}) = aLn(T_{cv}) + b\left[\begin{array}{l}\left(\frac{C}{T_{cv}}\right)\coth\left(\frac{C}{T_{cv}}\right)\\ -Ln\left(\sinh\left(\frac{C}{T_{cv}}\right)\right)\end{array}\right] - d\Bigg[\times\left(\frac{e}{T_{cv}}\right)\tanh\left(\frac{e}{T_{cv}}\right)\Bigg] \tag{47}$$

5. Numerical method

To achieve two independent thermodynamic properties, first law of thermodynamic, equation (4) and continuity equation of (6) should be used. These equations are discretize as:

$$u_{cv}^{j+1} = \frac{1}{m_{cv}^{j+1}}\left[\left(\frac{dQ_{cv}^j}{d\theta} - \frac{dW_{cv}^j}{d\theta} + \left(\frac{dm_s}{d\theta}\right)^j h_s - \left(\frac{dm_d}{d\theta}\right)^j h\right)\Delta\theta + m_{cv}^j u_{cv}^j\right] \tag{48}$$

$$m_{cv}^{j+1} = m_{cv}^j + \left(\left(\frac{dm_s}{d\theta}\right)^j - \left(\frac{dm_d}{d\theta}\right)^j\right)\Delta\theta \tag{49}$$

In these equations $\Delta\theta = 2\pi/n$ and n is the time steps. In this study, each degree of crank revolution is divided to 10 steps, then it can be said that 3600 data have been calculated for each thermodynamic property. Indicated work and Heat transfer discretization are achieved as:

$$W_{cv}^j = P_{cv}^j dV_{cv}^j \tag{50}$$

$$\dot{Q}_{cv}^j = \frac{1}{\omega}U_{cv}^j A_{cv}^j\left(T_{cv}^j - T_w\right) \tag{51}$$

In equation of (48), h_s and h_d are specific enthalpies of methane, which are calculated according to inlet and outlet conditions, respectively. By computing instantaneous specific internal energy, in-cylinder mass of gas and instantaneous volume of gas, according to below relation, instantaneous density of control volume at each crank revolution will be obtained:

$$\rho_{cv}^{j+1} = \frac{m_{cv}^{j+1}}{V_{cv}^{j+1}} \quad (52)$$

With these calculations, other thermodynamic properties will be measured. According to AGA8 EOS thermodynamic data, functions of pressure and temperature are prepared to compute them [36].

6. Genetic algorithm (GA) optimization

To obtain optimum timing events of RNGEE, genetic algorithm is used according to angles and inlet lap as parameters and exergy efficiency, equation (31), as fitness function. It means that with least exergy transfer to system, maximum power should be produced. Number of generation n_g, is used stopping criterion in this work. Roulette Wheel Selection (RWS) is used to compute fitness function. In the current study GA parameters are selected as: $n_s = 20$, $n_g = 700$, $p_c = 0.99$, $p_m = 0.1$, $p_r = 0.05$ and $r_c = 1$.

6.1. Objective parameters and boundaries

In whole valve configurations, port timing is an objective function, but in PVC and SVC, inlet lap is considered too. Upper and lower bounds of parameters should be defined to calculate fitness function. For optimization, boundaries of Table 1 are used.

6.2. The constraints

According to physical and thermodynamical restrictions, some constraints were used to obtain parameters. Firstly, it was considered that no back flow will occur during inlet and outlet periods in all valve styles except FVC. In FVC configuration constraint of having not back flow at the inlet process has been considered. In FVC style another constraint is used, since that there is one port to enter and exit of gas and it would be opened fully in both inlet and outlet processes unlike PVC style, the expansion process should be equal to compression process. A penalty factor is imposed to allow solutions to remain in the population during the solution progress, for example, if inlet mass back flow rate occurs, fitness function is multiplied to 10^6, evidently parameters at this condition won't be considered.

7. Results and discussion

In RNGEE, valve timing which means opening/closing port timing has a significant effect on engine performance events. Firstly, the effect of processes period on exergy destruction and power generation has been investigated, and then port timing has been optimized according to exergy efficiency as fitness function. GA has been considered as an optimization programming and four valves configuration have been modeled to control inlet and outlet port opening and closing. The events of inlet, expansion, outlet and compression of gas in clearance besides inlet/outlet reverse flows have been modeled too. Then P–V diagrams at each crank angle will be simulated. In all these valve styles, the computations have been started from the inlet port opening at the beginning piston motion at TDC. Pressure and temperature at the start of the inlet process were assumed during the first iteration, and the residual gas fraction was assumed to be as P_cV_c/ZRT_c. At the end of first iteration, thermodynamic properties have been calculated and the iteration is repeated until the convergence condition is obtained. These conditions are equality of temperature and pressure at the start and end of the cycle. For the analysis, MATLAB software has been used to measure in-cylinder gas properties and valve motions at various crank angles with engine parameters, Table 2.

Table 1
Boundaries of timing optimization.

style	bounds
PVC	$80^\circ \le \theta_c \le 130^\circ$
SVC	$10 \le S_l \le 50\ mm$
CVC	$60^\circ \le \theta_c \le 90^\circ$ $160^\circ \le \theta_c \le 200^\circ$ $320^\circ \le \theta_c \le 350^\circ$
FVC	$50^\circ \le \theta_c \le 90^\circ$ $90^\circ \le \theta_c \le 120^\circ$ $270^\circ \le \theta_c \le 310^\circ$

Table 2
Expansion Engine parameters.

Operating condition	Data	Operating condition	Data
P_s	40, 55 & 70 bars	D_i	18 cm
P_d	17 bars	D_v	4.5 cm
$n_b{*}w_b$	10×5 mm	T_s	300 K
W_p	3.5 cm	T_0	298 K
V_0	11% V_{dis}	f	0.2
L_r	0.5 cm	R	6 cm
N	750 rpm	L	40 cm

Table 3
Optimization results.

	θ_0	θ_i	θ_1	θ_2	θ_e	Inlet back	Outlet back
CVC	66	185	–	–	323	no	no
FVC	60	118	148	289	319	no	yes
SVC	$\theta_c = 101$		$S_l = 13\ mm$			no	no
PVC	$\theta_c = 100$		$S_l = 25\ mm$			no	no

7.1. Timing optimization results

In CVC and FVC, all port opening and closing time have been optimized, when in SVC and PVC, just IPCT has been optimized, as in these two valve styles, all events have been controlled according to cut-off angle. It should be mentioned that exhaust lap and lead are measured zero with GA, i.e. $E_l = L_e = 0$ and then inlet lap should be optimized too. In Table 3, results of optimization data are given. In CVC, inlet process should be ended at 66°, the beginning time of the outlet process is 185° and outlet port should be closed at 323° to start compression of residual mass. In FVC, IPCT is 60° and EPOT is 118°. Since of FVC geometry, EPFO is equal to EPOT plus half of IPCT, i.e. EPFO = EPOT + IPCT/2. For EPCT, this condition should be considered too. Cut-off angle for both SVC and PVC styles are almost equal, it is called 74% cut-off. But inlet lap of slide valve is shorter than a piston valve.

Except of FVC, in all styles, constraint of having not back flow in inlet and outlet periods has been achieved. According to Fig. 7, instantaneous port area of valves shows that in SVC and PVC, port cross section to enter the gas is not completely opened. EPOT and EPCT for slide and piston valve are obtained as 140 and 320° respectively.

According to geometrical configuration in slide valve, port width is measured as 1.8 cm which in piston valve, it is equal to 3.5 cm as CVC and FVC. In slide valve, port will be opened as 7 mm and in piston valve it will be opened as 14 mm for inlet process, but for an outlet period, port will be fully opened in both valves. Fig. 8 shows that indicator work of SVC and PVC is higher than two other styles. FVC produces least work and back flow is occurred during the outlet process in this type. There is another note from Fig. 7, there is the equality of expansion and compression period in SVC, PVC and FVC.

Power generation Table 4 shows the indicated power, friction and brake power of RNGEE based on total inlet mass. Results have

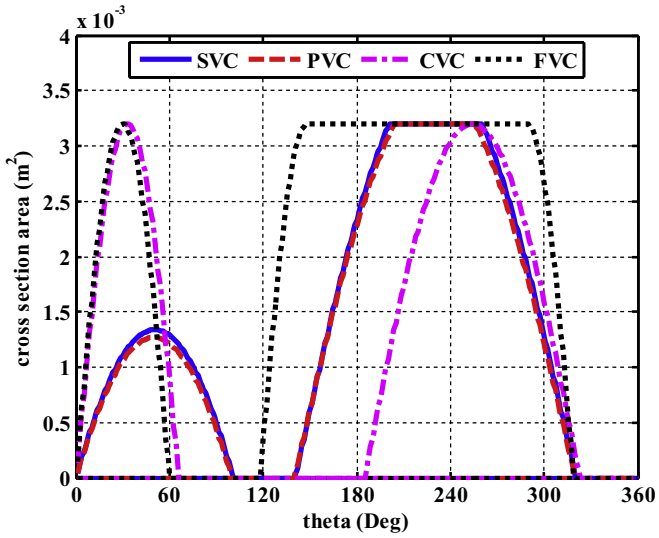

Fig. 7. Cross section area of port opening.

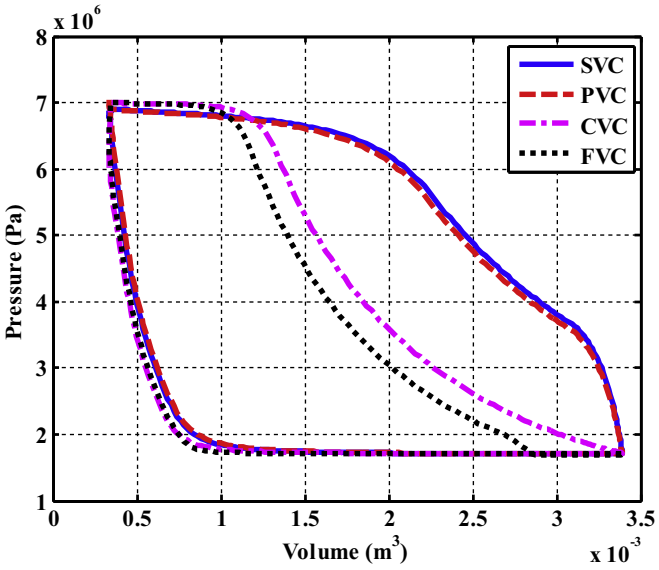

Fig. 8. Indicator diagram of valves.

been showed that although indicated power, area of the pressure-volume diagram, in SVC is higher than other valve styles, but according to entire inlet mass, CVC and FVC produced more power. Since, friction power based on total mass transfer in FVC is more than CVC, brake power, output power of RNGEE, in case of CVC is at its highest value. Inlet period in SVC is more than others, so it can be seen that it has total mass flow rate of 1 kg/s.

7.2. Exergy analysis

An exergy analysis of an RNGEE has been carried out to obtain the engine's efficiency which is called exergy efficiency here. Applying second law of thermodynamics besides the first law represents the results of entropy generation and exergy destruction of the pressure reduction process of NG. Instantaneous variations of exergy destruction sources due to heat transfer, mixing, inlet/outlet throttling and friction in CVC and FVC is the same. This behavior is happened in SVC and PVC too. So variations of these parameters are just compared according to CVC and PVC in following. Through Figs. 9–12, from the second-law analysis point of view, results

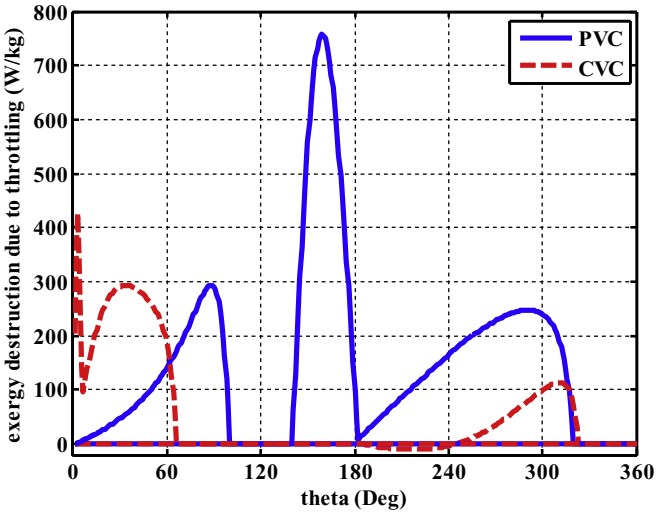

Fig. 9. Exergy destruction due to throttling.

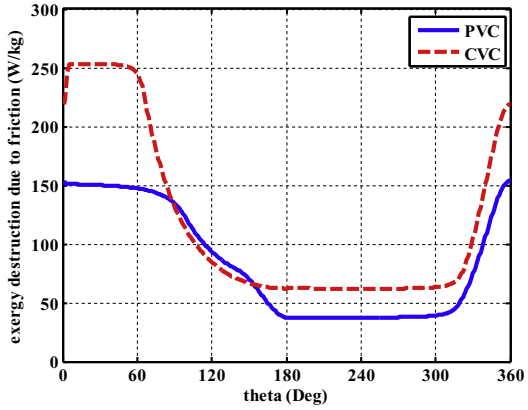

Fig. 10. Exergy destruction due to friction.

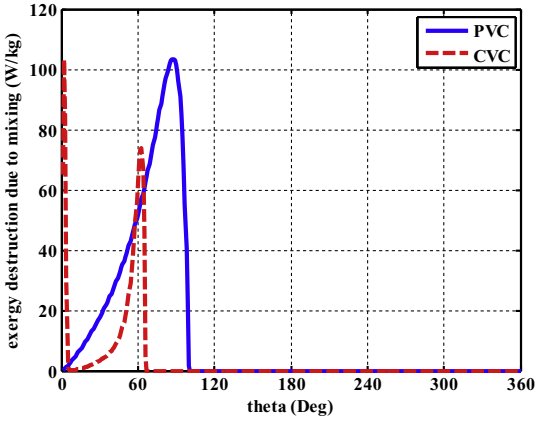

Fig. 11. Exergy destruction due to mixing.

showed that in each cycle, outlet throttling, inlet throttling, friction, mixing and heat transfer causes more exergy destruction respectively. In Fig. 9, the two left curves are related to inlet throttling, and two right curves are related to outlet throttling. Fig. 10 shows that friction power will be decreased in the outlet process in all valve styles. There is one other thing that friction in PVC and SVC is less than CVC and FVC, because pressure loss through gas passage in later cases is more than other styles. Exergy destruction, due to

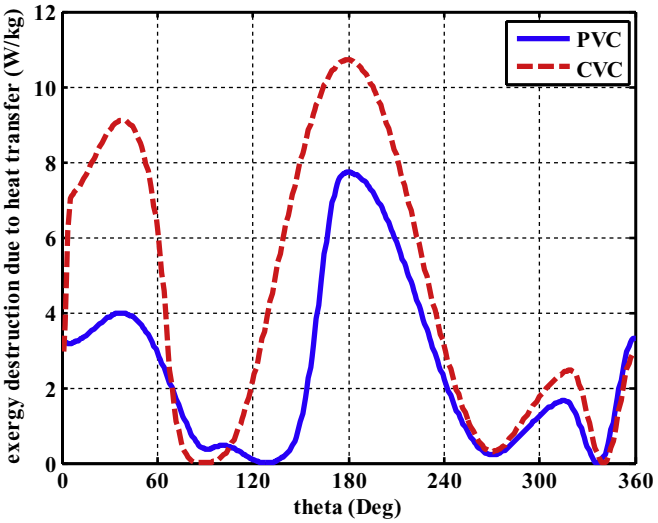

Fig. 12. Exergy destruction due to heat transfer.

mixing in PVC because of more inlet periods, is higher than CVC, Fig. 11. According to Fig. 12, exergy destruction due to heat transfer could be neglected.

By integration of each exergy destruction in one cycle from following chart it was obtained that in slide and piston valve styles, a and b in Fig. 13, exergy lost due to releasing the gas has more effect than other exergies lost sources, 65% in SVC and 62% in PVC. Inlet throttling has second effect on exergy destruction in these two styles. But importance of exergy destruction due to these sources in CVC and FVC is contrary to piston and slide valves. It means that in CVC and FVC styles, inlet throttling has more effect rather than outlet throttling on exergy lost. For example, in CVC, 45% for inlet and 12% for outlet, plot c in Fig. 13. This phenomenon can be achieved from Fig. 14 which pressure difference between supply line and in-cylinder gas at piston and slide valves is very little, but in flange and cylinder valves, there is almost 10 bar difference between them in the inlet period. In CVC and FVC pressure of gas is begun from almost 60 bar when in other two valve configurations it is begun from 69 bar. Then according to equation (40), exergy destruction due to inlet throttling will be high. This is also true in outlet gas, it means that from EPOT to a degree of 180, the difference between gas pressure and discharge line pressure in SVC and PVC is higher than CVC and FVC.

In this study just the friction between cylinder and piston has been considered. Effect of friction power on exergy destruction in cylinder and flange valves is significantly more than piston and slide valves. Exergy destruction due to heat transfer is more than effect of mixing in CVC and FVC, but in piston and slide valves is contrary. Timing optimization of flange valve is achieved under back flow conditions at the outlet process, it can be seen from Fig. 15 that just in this valve configuration, back flow will occur in a cycle.

In Table 5, data of exergy destruction sources of valve styles are

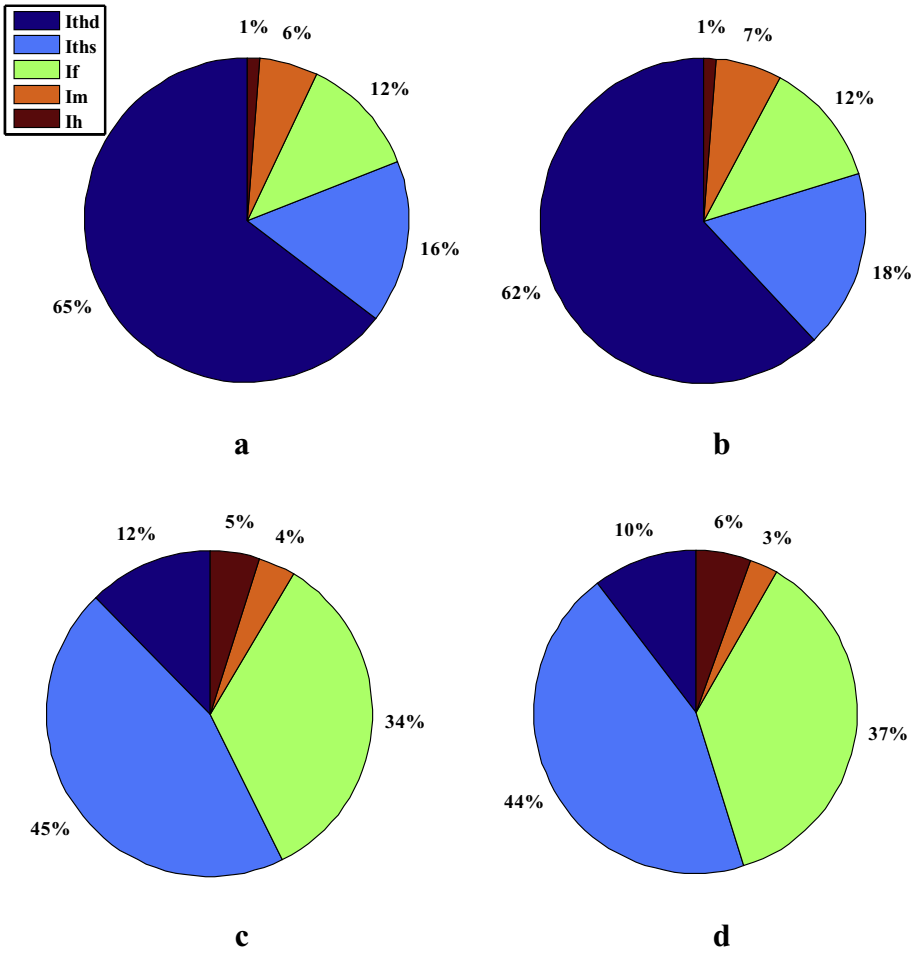

Fig. 13. Exergy destruction sources, a: SVC, b: PVC, c: CVC and d: FVC.

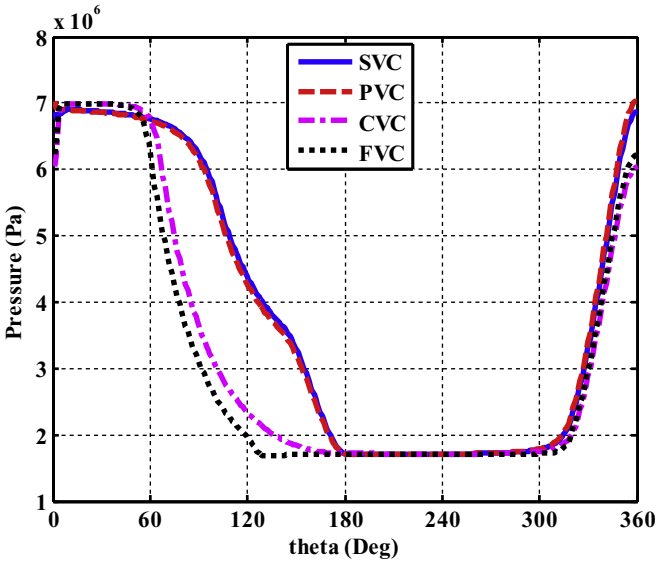

Fig. 14. Pressure variations.

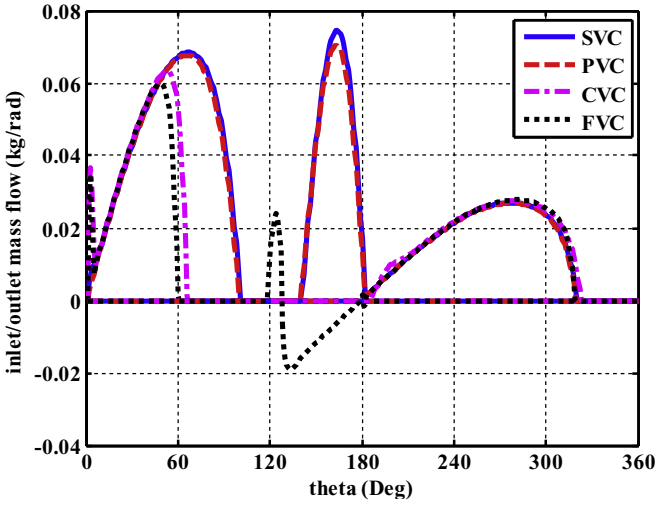

Fig. 15. Inlet/outlet mass flow rate.

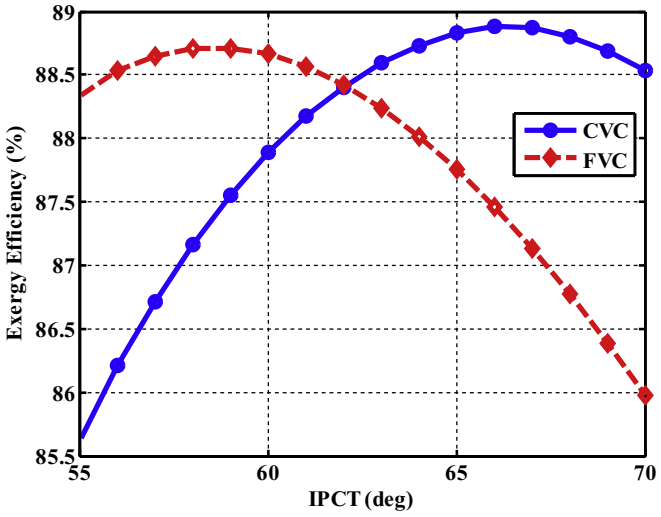

Fig. 16. Effect of IPCT on exergy efficiency of CVC and FVC.

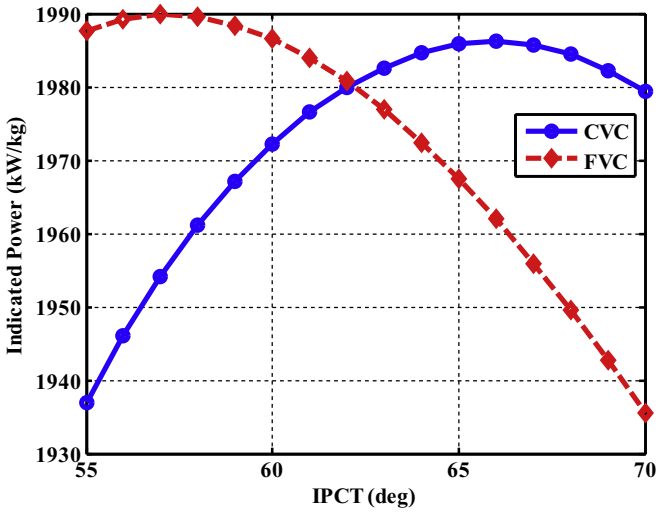

Fig. 17. Effect of IPCT on indicated power of CVC and FVC.

given. It can be seen that exergy destruction due to heat transfer and mixing could be neglected because of their low impact, similar results were obtained in compressors [16].

7.3. Effect of timing variation on exergy destruction and power generation

In this section, effect of timing variation on engine performance will be shown. Figs. 16 and 17 show that according to optimization

Table 4
Power generation results.

	$\dot{m}$ (kg/s)	$\dot{m}_s$ (kg)	$\dot{W}_{ind}$ (kW)	$\dot{W}_{ind_m}$ (kW/kg)	$\dot{W}_{fr_m}(kW/kg)$	$\dot{W}_{b_m}(kW/kg)$
CVC	0.59	0.047	93	1986.3	118.5	1867.8
FVC	0.5	0.04	78.8	1986.5	134.5	1852
SVC	1	0.08	139	1745.9	82	1663.9
PVC	0.97	0.078	135.8	1753.2	84.1	1669.1

Table 5
Data of exergy lost sources.

	$\dot{I}_{th_s}$ (kW/kg)	$\dot{I}_{th_d}$ (kW/kg)	$\dot{I}_{fr}(kW/kg)$	$\dot{I}_h(kW/kg)$	$\dot{I}_m(kW/kg)$
CVC	155.8	42.2	118.5	16.2	12
FVC	162.3	39	134.5	19.1	10.9
SVC	111.7	442.3	82	8.6	40.3
PVC	120.4	418.8	84.1	8.9	43.3

of IPCT as 66° for CVC and 60° for FVC, inlet period affects exergy efficiency and indicated power significantly. For example, if IPCT is occurred at 55°, the RNGEE will produce power of 1938 kW/kg, where at the optimized time, it produces 1986 kW/kg of power. From 55 until 66° power generation of CVC is increased and after that it will be decreased. In FVC almost in all time, increasing inlet period of gas will cause to decline of power. This behavior has been seen on exergy destruction too.

Figs. 18 and 19 show that power generation, exergy efficiency and all exergy destruction of engine, FVC and CVC styles, won't be influenced by the exhaust port opening time. It just has a low impact on exergy destruction due to inlet throttling, so that it varies from 63 to 23 kW/kg with increasing of EPOT. This phenomenon is happened on closing time of outlet port too, Figs. 20 and 21. The effect of EPCT in CVC is lower than FVC. In FVC, indicated power is equal to 1981 kW/kg at 315° and 1975 at 330°. But in CVC, it begins from 1985 to 1962 kW/kg. There is a fantastic proposition in power generation and exergy efficiency of these two engine valve styles based on optimized closure time of FVC. In degree of 319, both CVC and FVC have an equal value of power generation and exergy destruction. But based on optimized time of CVC, 323°, FVC produces less power than CVC.

It was obtained that according to selected engine parameters, by variation of cut-off angle from 80 to 110° of crank revolution, in SVC exergy efficiency will be increased from 78.5% in 80° to 79% in degree of 85 and then will be declined to 71% in degree of 110.

This was happened in PVC too, Fig. 22, from 78.2 to 78.8% firstly, and to 71% secondly. Indicated power has been changed from almost 1800 to 1670 kW/kg in both cases like the behavior of exergy efficiency, Fig. 23. According to these figures, the best time for cut-off angle is 85° of crank revolution, but since that an important constraint of having no back flow in both inlet and outlet processes has been considered, this time is optimized at degree of 100. It means that before this time, back flow will be occurred at inlet and outlet the gas. Because the compression period of gas will be raised and then the pressure of residual gas will be increased too.

Finally, results showed that variation of inlet lap does not affect power generation and exergy efficiency, but through Figs. 24 and 25, it can be achieved that this parameter can impact on exergy destruction sources of inlet and outlet throttling and some low on mixing.

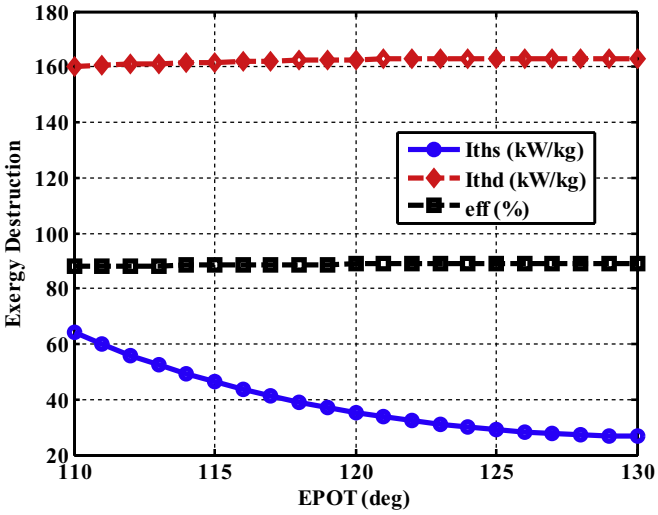

Fig. 19. Effect of EPOT on exergy destruction of FVC.

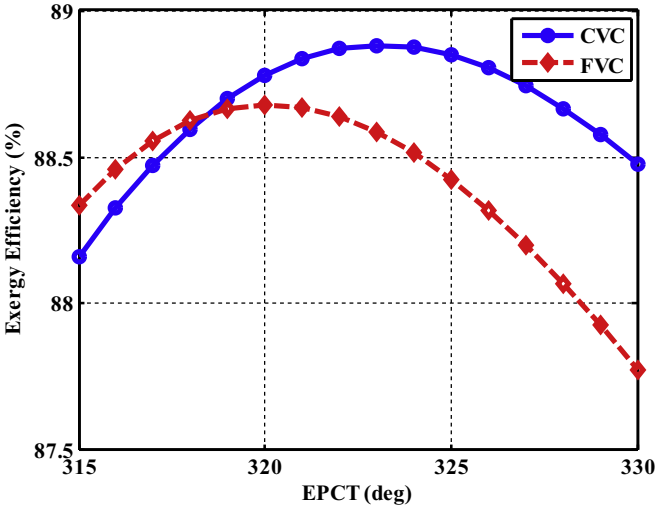

Fig. 20. Effect of EPCT on exergy efficiency of CVC and FVC.

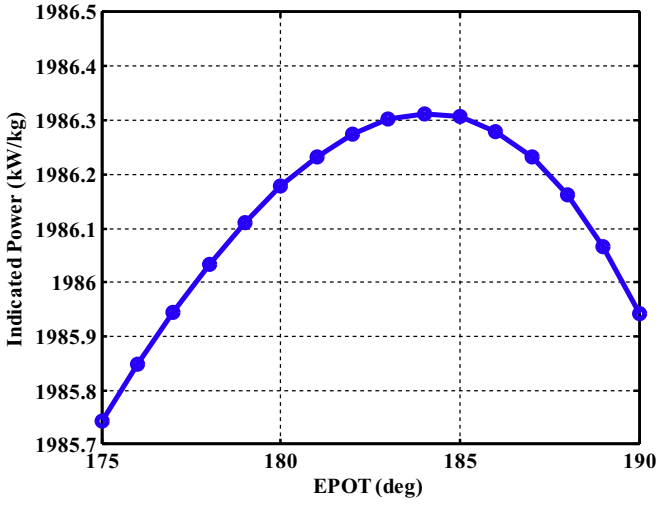

Fig. 18. Effect of EPOT on indicated power of CVC.

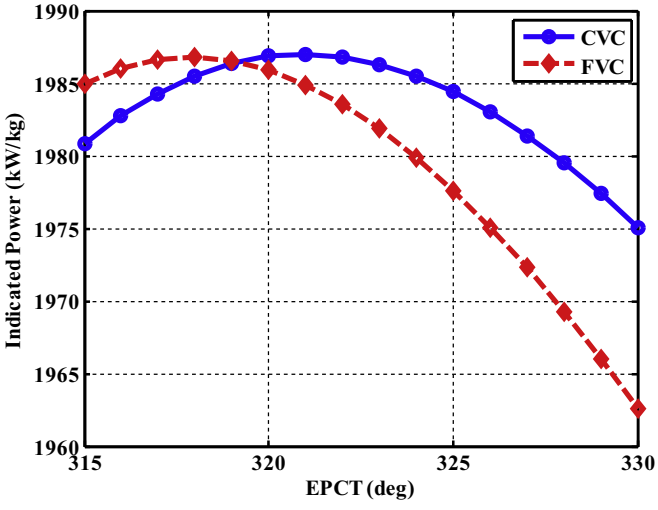

Fig. 21. Effect of EPCT on indicated power of CVC and FVC.

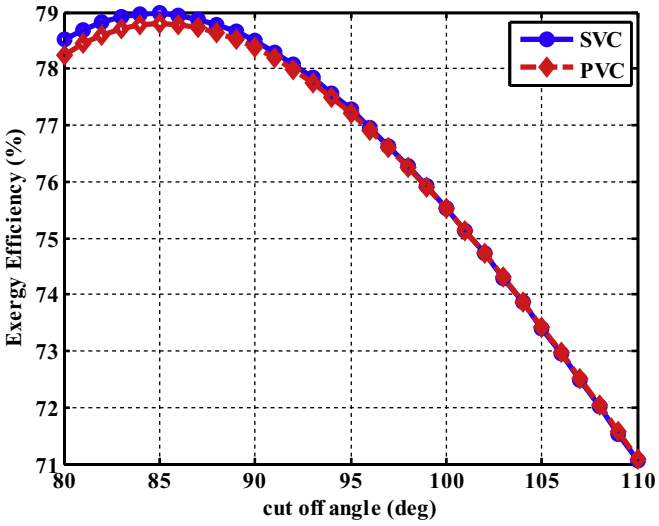

Fig. 22. Effect of cut-off angle on exergy efficiency of SVC and PVC.

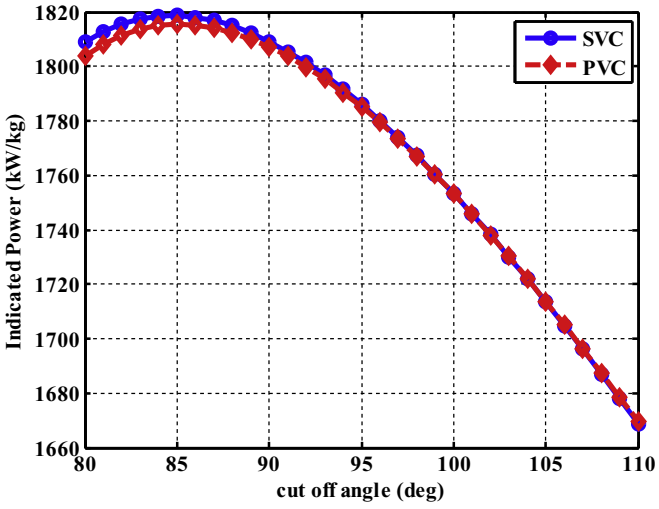

Fig. 23. Effect of cut-off angle on indicated power of SVC and PVC.

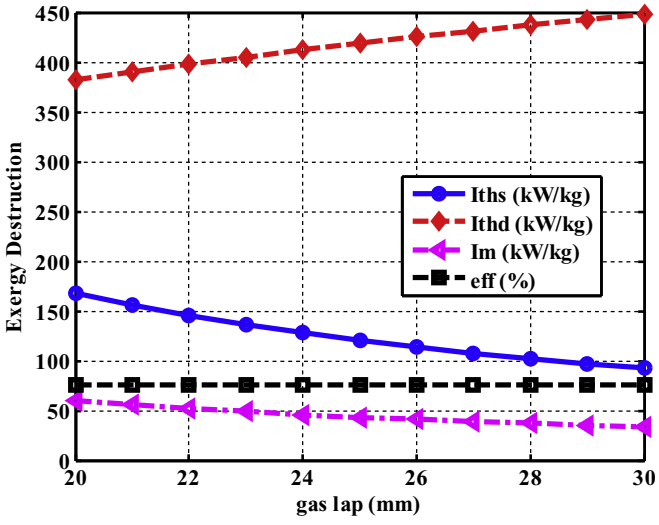

Fig. 24. Effect of inlet lap on exergy destruction of PVC.

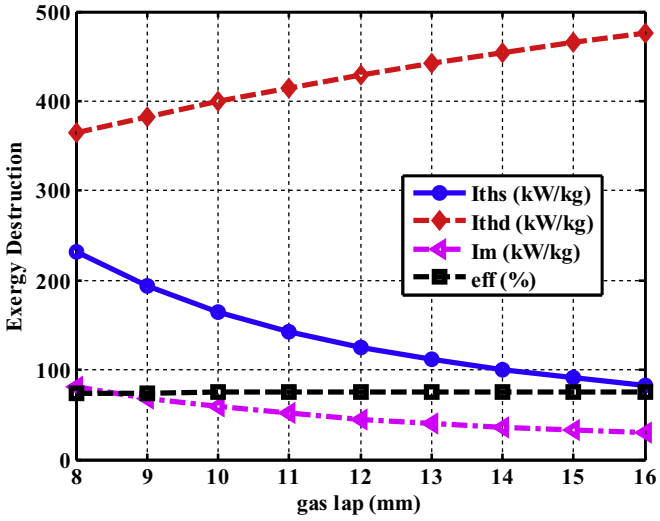

Fig. 25. Effect of inlet lap on exergy destruction of SVC.

7.4. Effect of NG pressure supply line variation on exergy efficiency and power generation

Fig. 26 shows the effect of NG inlet pressure to RNGEE in all valve styles. As it is seen, an increase in NG supply pressure, from 30 to 70 bars, has more effect on the exergy efficiency of cylinder and flange valve, it rises from 19.8 to 88.9% in CVC and 4.1–88.7% in FVC. It can be seen that increasing inlet pressure will decrement exergy efficiency of the engine in slide and piston valve styles from 84.8 to 75.5%.

Fig. 27 is given to clarify the effect of natural gas pressure variation in supply line on engine power generation. As it can be shown, an increase in pressure supply line leads to a positive impact RNGEE output power in all valve styles which increases from 626.4 to 1663.8 kW/kg in piston and slide valves and from −58 to 1867.8 kW/kg in cylinder valve and finally from −315.7–1852 kW/kg in flange valve. Indeed, if the cylinder and flange valve styles are used instead of expansion valve with the pressure supply line of 30 bar, the system of RNGEE Should be removed from the gas pressure reduction circuit and the circuit of expansion valve should be used. For using of an engine in all

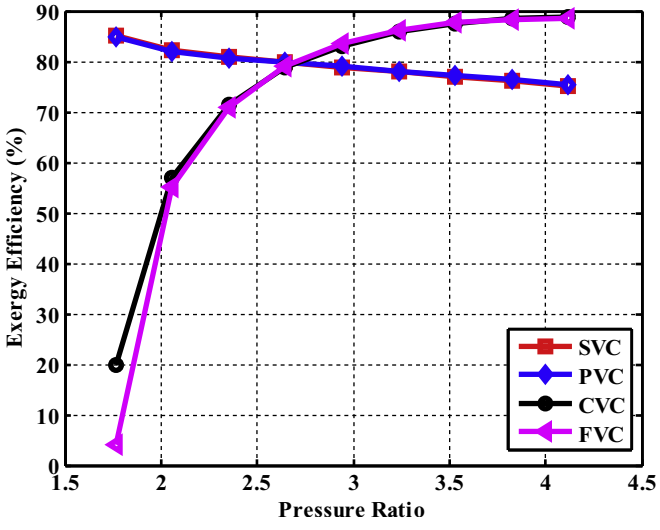

Fig. 26. Effect of supply line pressure variation on exergy efficiency.

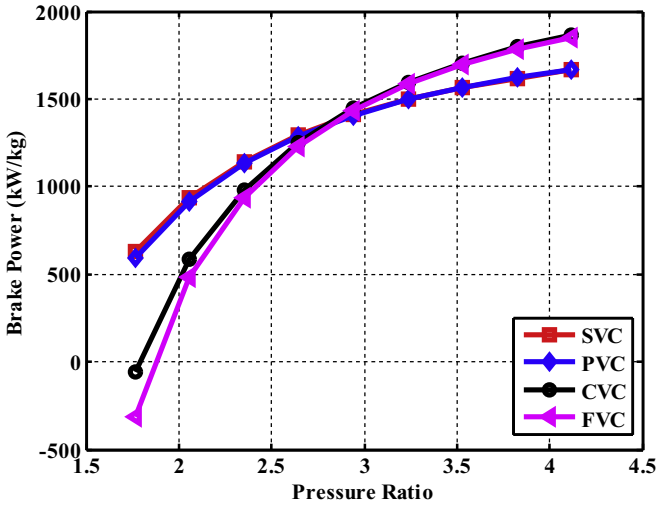

Fig. 27. Effect of supply line pressure variation on output power.

conditions even at the condition of inlet pressure of 30 bar and lower, it can be used the time variable of an engine. It means that cut-off angle of an engine is set according to pressure supply line. Because according to above results, it can be said that engine performance is depended on the cut-off angle more than other angles.

8. Conclusion

Potential pressure energy of high-pressure natural gas is destroyed while using throttling valve to decrease its pressure in natural gas (NG) pressure drop stations. As a results there is possibility of using such a device to recover the pressure energy of the gas. Reciprocating natural gas expansion engine (RNGEE) is among of such devices. So a RNGEE could be employed in parallel with throttling valves to recover pressure energy during the reduction and expansion of high-pressure NG and to transfer mechanical work into electrical energy.

In RNGEE, ports are used instead of valves to enter and exit the gas. Port timing is one of the most important parameters, which has a major effect on the RNGEE operation. To maximize RNGEE power generation, a numerical model is developed based on the first and second law of thermodynamics to optimize opening/closure time of ports using genetic algorithm. Four types of valve are considered and exergy efficiency is used as a fitness function for time optimization. Results showed that valve configuration and port timing has a significant effect on power generation and exergy loss in RNGEE. According to results, it can be concluded that the stopping inlet time of gas has the most effect on the power generation. According to constraints intended, inlet period in SVC (slide valve configuration) and PVC (piston valve configuration) is higher than others. Although indicated power in SVC and PVC is more than FVC (flange valve configuration) and CVC (cylinder valve configuration), but based on total inlet mass, latter valves produces more power. It should be said that FVC produces less power than CVC, 78.8 against 93 kW. Exergy analysis showed that the effect of mixing and heat transfer on exergy destruction is lower than friction and throttling. Friction power in FVC and CVC is higher than two other valves. Results showed that exergy destruction due to outlet throttling has its lowest value in SVC and its highest value is occurred at FVC. Therefore exergy destruction due to inlet throttling has an opposite behavior. Port timing showed that θ_i has no effect on engine performance and the effect of θ_e on power producing at FVC is higher than CVC, although it doesn't more effect on exergy efficiency.

Based on optimum values for inlet lap and cut-off angle, the behavior of SVC and PVC was obtained equal. Inlet lap affects seriously on exergy destruction due to inlet and outlet throttling. The effect of NG pressure supply line showed that at inlet pressure condition of 30 bar, according to negative power generation, RNGEE with CVC and FVC should not be used.

References

[1] Kostowski WJ, Usón S. Thermoeconomic assessment of a natural gas expansion system integrated with a co-generation unit. Appl Energy 2013;101:58–66.
[2] Sanaye S, Nasab AM. Modeling and optimizing a CHP system for natural gas pressure reduction plant. Energy 2012;40:358–69.
[3] Sanaye S, Nasab AM. Modeling and optimization of a natural gas pressure reduction station to produce electricity using genetic algorithm. In: Andea P, Kilyeni S, editors. 6th wseas international conference on energy, environment, ecosystems and sustainable development. Romania: Politehnica University of Timisoara; 2010. p. 62–70.
[4] Badr O, Naik S, O'Callaghan PW. Expansion machine for a low power-output Steam Rankine – cycle engine. Appl Energy 1991;39:93–116.
[5] Farzaneh-Gord M, Arabkoohsar A, Deymi Dasht-bayaz M, Machado L, Koury RNN. Energy and exergy analysis of natural gas pressure reduction points equipped with solar heat and controllable heaters. Renew Energy 2014;72:258–70.
[6] Bisio G. Thermodynamic analysis of the use of pressure exergy of natural gas. J Exergy 1995;20:161–7.
[7] Neseli MA, Ozgener O, Ozgener L. Energy and exergy analysis of electricity generation from natural gas pressure reducing stations. Energy Convers Manag 2015;93:109–20.
[8] Usón S, Kostowski WJ. Integrating an ORC into a natural gas expansion plant supplied with a co-generation unit. In: The 25th international conference on efficiency, cost, optimization, simulation and environmental impact of energy systems, Perugia, Italy, June 26–29; 2012.
[9] Kolasiński P, Pomorski M, Błasiak P, Rak J. Use of rolling piston expanders for energy Regeneration in natural gas pressure reduction stations—selected thermodynamic issues. Appl Sci 2017;7(no. 6):535–52.
[10] Dehli M. Concepts of gas expansion at high temperature. Netherland: MECC Maastricht; 1997. p. 16.
[11] Farzaneh-Gord M, Jannatabadi M. Simulation of single acting natural gas Reciprocating Expansion Engine based on ideal gas model. J Nat Gas Sci Eng 2014;21:669–79.
[12] Farzaneh-Gord M, Jannatabadi M. Timing optimization of single-stage single-acting reciprocating expansion engine based on exergy analysis. Energy Convers Manag 2015;105:518–29.
[13] Farzaneh-Gord M, Izadi S, Deymi-Dashtebayaz M, Pishbin SI. Optimizing natural gas reciprocating expansion engines for Town Border pressure reduction stations based on AGA8 equation of state. J Nat Gas Sci Eng 2015;26:6–17.
[14] Bejan A. Fundamentals of exergy analysis, entropy generation minimization and the generation of flow architecture. Int J Energy Res 2002;26(7):545–65.
[15] McGovern JA, Harte S. An exergy method for compressor performance analysis. Int J Refregerat 1995;18(6):421–33.
[16] McGovern JA, Harte S. Computer simulation of exergy destruction withina reciprocating compressor. In: International compressor engineering conference, Purdue; 1992.
[17] Qiu G, Liu H, Riffat S. Expanders for micro-CHP systems with organic Rankine cycle. Appl Therm Eng 2011;31:3301–7.
[18] Lee S. First law analysis of unsteady processes with application to charging process and a reciprocating compressor. M.S. thesis. Ohio State Univesity; 1983. p. 143.
[19] Oosthuizen P, Carscallen W. Compressible fluid flow. United State of America: McGraw-Hill; 1997. p. 179–224.
[20] Standard B. Measurement of fluid flow by means of pressure differential devices inserted in circular cross-section conduits running full. EN ISO; 2003. p. 5167–72.
[21] Hall WB, Eng FR, Mech FIE. Predicting locomotive performance. 1998.
[22] Tchanche BF, Lambrinos Gr, Frangoudakis A, Papadakis G. Exergy analysis of micro-organic Rankine power cycles for a small scale solar driven reverse osmosis desalination system. Appl Energy 2010;87:1295–306.
[23] Wall G. Exergy conversion in the Japanese Society. Energy 1995;15:435–44.
[24] Cowden R, Nahon M, Rosen MA. Exergy analysis of a fuel cell power system for transportation applications. Int J Exergy 2001;2:112–21.
[25] Cerci Y. Exergy analysis of a reverse osmosis desalination plant in California. Desalination 2002;142:257–66.
[26] Ally MR, Munk JD, Baxter VD, Gehl AC. Exergy analysis of a two-stage ground source heat pump with a vertical bore for residential space conditioning under simulated occupancy. Appl Energy 2015;155:502–14.
[27] Bejan A, Tsatsaronis G, Moran M. Thermal design and optimization. New York: Wiley; 1996.
[28] Wylen G, Sonntag R. Fundamentals of classical thermodynamics. New York: Wiley; 1976.

[29] Kotas TJ. The exergy method of thermal plant analysis. London: Butterworths; 1985.
[30] Tsatsaronis G. Thermoeconomic analysis and optimization of energy systems. Prog Energy Combust Sci 1993;19(3):227–57.
[31] Szargut J, Morris DR, Steward FR. Exergy analysis of thermal, chemical, and metallurgical processes hemisphere. New York: Publishing Corporation; 1988.
[32] Farzaneh-Gord M, Rahbari HR. Numerical procedures for natural gas accurate thermodynamics properties calculation. J Eng Thermophys 2012;21(4):213–34.
[33] AGA8–DC92 EoS. Compressibility and super compressibility for natural gas and other hydrocarbon gases. 1992. Committee Report No. 8, AGACatalog No. XQ 1285, Arlington,VA.
[34] Moran MJ, Shapiro HN. Fundamentals of engineering thermodynamics. New York: Wiley; 2007.
[35] DIPPR@ 801. Evaluated standard thermophysical property values, design institute for physical properties, sponsored by AIChE. 2004.
[36] Farzaneh-Gord M, Rahbari HR. Developing novel correlations for calculating natural gas thermodynamic properties. Chem Process Eng 2011;32(4):435–52.

Nomenclature

A: port area (m^2)
b: specific flow exergy function(kW)
C_d: coefficient of discharge
C_P: constant pressure specific heat$(j/kg.K)$
D_i: piston diameter(m)
D_v: valve diameter (m)
E_l: exhaust lap (m)
f: friction factor
h: specific enthalpy(j/kg)
$\dot{I}$: exergy destruction(kW)
L: connecting rod length(m)
L_p: port length (m)
L_e: lead (m)
L_r: ring wide(m)
$\dot{m}$: mass flow rate (kg/s)
N: motor speed(rpm)
n_b: number of bridges
n_s: number of population
n_g: number of generation
P: pressure (pa)
p_c: crossover
p_m: mutation
p_r: probability
$\dot{Q}$: heat transfer rate (kW)
R: crank radius(m)
R_g: constant coefficient of methane$(j/kg.K)$
R_i: inside convection resistance (w/K)
r_{eq}: eccentric crank radius (m)
r_p: pressure ratio
S: engine course(m)
$\dot{S}_{gen}$: entropy generation(W/K)
S_l: inlet lap (m)
s: specific entropy $(j/kg.K)$
s'_s: specific entropy after throttling$(j/kg.K)$
T: temperature(K)
t: time (sec)
U: overall heat transfer coefficient $(w/m^2.K)$
V: volume(m^3)
W: power(kW)
w_b: bridge width (m)
x: piston displacement (m)
y_i: Inlet port opening (m)
y_o: outlet port opening (m)
z: valve displacement (m)
Z: compressible factor

Greek symbols

γ: isentropic power
Ψ: exergy efficiency
$\dot{\Xi}_t$: rate of exergy transfer(kW)
ω: rotational speed (rad/s)
ψ: eccentric angle of advance
ρ: density $(kmol/m^3)$
θ_0: intake port closure time (IPCT)
θ_i: exhaust port opening time (EPOT)
θ_e: exhaust port closure time (EPCT)
θ_1: time of fully opened exhaust port (EPFO)
θ_2: time of exhaust port begins to close (EPBC)
θ_c: cut-off angle
θ: instant angle of connecting rod(deg)

Subscripts

cl: clearance volume
b: brake work
cv: control volume of expansion engine
d: outlet
f: friction
m: molar
ds: down stream
r: Reduced
mix: refer to mixing
Q: refer to heat transfer
s: suction
th: refer to throttling
w: wall cylinder
us: up stream
0: Dead state